Discrete and continuum phenotype-structured models for the evolution of cancer cell populations under chemotherapy

Math. Model. Nat. Phenom. 15 (2020) 14
https://doi.org/10.1051/mmnp/2019027

Mathematical Modelling of Natural Phenomena
www.mmnp-journal.org

DISCRETE AND CONTINUUM PHENOTYPE-STRUCTURED MODELS FOR THE EVOLUTION OF CANCER CELL POPULATIONS UNDER CHEMOTHERAPY*

Rebecca E.A. Stace[1], Thomas Stiehl[2], Mark A.J. Chaplain[3], Anna Marciniak-Czochra[4] and Tommaso Lorenzi[5,**]

Abstract. We present a stochastic individual-based model for the phenotypic evolution of cancer cell populations under chemotherapy. In particular, we consider the case of combination cancer therapy whereby a chemotherapeutic agent is administered as the primary treatment and an epigenetic drug is used as an adjuvant treatment. The cell population is structured by the expression level of a gene that controls cell proliferation and chemoresistance. In order to obtain an analytical description of evolutionary dynamics, we formally derive a deterministic continuum counterpart of this discrete model, which is given by a nonlocal parabolic equation for the cell population density function. Integrating computational simulations of the individual-based model with analysis of the corresponding continuum model, we perform a complete exploration of the model parameter space. We show that harsher environmental conditions and higher probabilities of spontaneous epimutation can lead to more effective chemotherapy, and we demonstrate the existence of an inverse relationship between the efficacy of the epigenetic drug and the probability of spontaneous epimutation. Taken together, the outcomes of the model provide theoretical ground for the development of anticancer protocols that use lower concentrations of chemotherapeutic agents in combination with epigenetic drugs capable of promoting the re-expression of epigenetically regulated genes.

Mathematics Subject Classification. 92B05, 92-08, 35Q92, 35B40.

Received January 31, 2019. Accepted June 17, 2019.

1. Introduction

Mathematical modelling can contribute to cancer research by supporting experimental results with a theoretical basis. Furthermore, mathematical models can generate new experimentally testable hypotheses which can

* T.S. and A.M.-C. were supported by research funding from the German Research Foundation DFG (SFB 873; subproject B08). T.L. gratefully acknowledges support from the Heidelberg Graduate School.

Keywords and phrases: Cancer cell populations, chemotherapy, epigenetic drugs, individual-based models, nonlocal parabolic equations.

[1] School of Mathematics and Statistics, University of St Andrews, North Haugh, St Andrews, Fife KY16 9SS, UK.
[2] Institute of Applied Mathematics, Im Neuenheimer Feld 205, Heidelberg University, 69120 Heidelberg, Germany.
[3] School of Mathematics and Statistics, University of St Andrews, North Haugh, St Andrews, Fife KY16 9SS, UK.
[4] Institute of Applied Mathematics, BIOQUANT and IWR, Im Neuenheimer Feld 205, Heidelberg University, 69120 Heidelberg, Germany.
[5] School of Mathematics and Statistics, University of St Andrews, North Haugh, St Andrews, Fife KY16 9SS, UK.

** Corresponding author: tl47@st-andrews.ac.uk

ultimately reveal emergent phenomena that would otherwise remain unobserved [3, 5–7, 17, 22, 36]. Amongst others, integro-differential equations and nonlocal partial differential equations (PDEs) modelling evolutionary dynamics in populations structured by physiological traits have provided fresh insight into how the adaptation of cancer cell populations exposed to antiproliferative drugs can be acted upon by selective pressures, which drive the outgrowth of drug-resistant phenotypic variants [2, 25–27, 29, 50–52, 54–56, 71].

A key advantage of these deterministic continuum models over their stochastic individual-based counterparts (*i.e.* discrete models that track the phenotypic evolution of single individual cells) is that they are amenable to mathematical analysis. This enables a complete exploration of the model parameter space, allowing more robust conclusions to be drawn. Furthermore, compared to individual-based models, such continuum models offer the possibility to carry out numerical simulations for large numbers of cells, while keeping computational costs within acceptable bounds. However, continuum models are defined at the scale of the whole cell population and, as such, they are usually formulated on the basis of phenomenological considerations. This can hinder a precise mathematical description of crucial evolutionary aspects. On the contrary, stochastic individual-based models describe the phenotypic evolution of single cells in terms of algorithmic rules, which can be more easily tailored to capture fine details of cellular dynamics. Therefore, such discrete models make it possible to achieve a more accurate mathematical representation of evolutionary dynamics in cancer cell populations. Furthermore, individual-based models are able to reproduce the emergence of population-level phenomena that are induced by stochastic fluctuations in single-cell phenotypic properties – which are relevant in the regime of low cell numbers and cannot easily be captured by continuum models. Therefore, it is desirable to derive continuum models for the response of cancer cell populations to chemotherapy as the appropriate limit of discrete models for the phenotypic evolution of single cells. This may provide a clearer picture of the modelling assumptions made and ensure they correctly reflect the essentials of the underlying biological problem.

In light of these considerations, aiming to complement the existing literature on phenotype-structured models of evolutionary dynamics in cancer cell populations, we present here a stochastic individual-based model for the phenotypic evolution of cancer cells under chemotherapy. In particular, we consider the case of combination cancer therapy whereby a chemotherapeutic agent is administered as the primary treatment and an epigenetic drug is used as an adjuvant treatment. The cancer cell population is structured by the expression level of a gene that controls both cell proliferation and chemoresistance, and the level of expression of this gene determines the cell phenotypic state. Each single cell within the population undergoes spontaneous epimutations and divides or dies according to a set of simple rules, which result in a discrete-time branching random walk on the space of phenotypic states. We formally derive a deterministic continuum counterpart of this discrete model, which we show to consist of a nonlocal parabolic PDE for the cell population density function (*i.e.* the cell distribution over the space of phenotypic states) [65]. Analysing the long-term behaviour of the solution to this equation, we obtain a precise qualitative and quantitative depiction of evolutionary dynamics in the cancer cell population. In this respect, our work follows earlier papers about the derivation of deterministic continuum models for the evolution of populations structured by physiological traits from stochastic individual-based models [19, 20, 23]. It also follows previous articles on the analysis of nonlocal parabolic PDEs with advection terms that arise from the mathematical modelling of adaptive dynamics in asexual populations [23, 24, 53].

Combining computational simulations of the individual-based model with analysis of the corresponding PDE, we perform a complete exploration of the model parameter space. In summary, the mathematical results obtained support cancer research by addressing the following questions:

Q1 How do chemotherapeutic agents shape the phenotypic composition and the size of cancer cell populations by interfering with the evolution of individual cells?
Q2 What conditions on single cells' evolutionary parameters underpin successful chemotherapy?
Q3 How does the efficacy of adjuvant epigenetic therapy relate to the probability for cancer cells to undergo spontaneous epimutation and to the dose of chemotherapy in use?
Q4 Can anticancer protocols that use lower concentrations of chemotherapeutic agents in combination with epigenetic drugs be more effective than therapeutic protocols based solely on high-dose chemotherapy?

The rest of the paper is organised as follows. In Section 2, we briefly describe the underlying biological problem and introduce the phenotype-structured individual-based model. In Section 3, we carry out a formal derivation of the corresponding deterministic continuum model and we study the long-time asymptotic behaviour of its solution, in order to achieve a precise mathematical characterisation of evolutionary dynamics within the cancer cell population. In Section 4, we present the results of computational simulations of the individual-based model, we integrate them with the analytical results established in Section 3, and we discuss their biological implications. Section 5 concludes the paper and provides a brief overview of possible research perspectives.

2. Biological background and description of the model

2.1. Biological background

Recent experimental and clinical studies indicate that carcinogenesis can be viewed as an evolutionary process at the cellular level [39, 45, 46, 58, 61, 73, 83, 85, 86, 88]. In summary, novel phenotypic variants emerge via heritable variations in gene expression. The existing phenotypic variants undergo natural selection through competition for space and resources, in some cases under the action of xenobiotic agents such as anticancer drugs, and the cells in fittest phenotypic states survive to proliferate at the expense of the weaker phenotypic variants.

Under such an evolutionary perspective, the development of chemoresistance in cancer cell populations can be conceptualised as a population bottleneck owing to the selective pressure exerted by the chemotherapeutic agent(s) in use. This is illustrated by the schematic diagram presented in Figure 1. Prior to chemotherapy, the cell population is mainly composed of highly-proliferating phenotypic variants, which have a competitive advantage over cells in slow-proliferating phenotypic states in favourable environmental conditions. Some slow-proliferating cells are still present because of genotypic and phenotypic variability. In the presence of chemotherapy, the population is exposed to the selective stress induced by the chemotherapeutic agent(s), which target mostly rapidly proliferating phenotypic variants. Therefore, cells with a lower proliferative potential will acquire a competitive advantage over more proliferative cells. As a result, most of the fast-proliferating, chemosensitive cells will die out and the aftermath of chemotherapy will be a population of slow-proliferating, chemoresistant cells. Hence, one will initially observe a reduction in the size of the cell population. However, since those cells that have survived chemotherapy will no longer respond to the therapeutic agents in use, and they will not have to compete anymore for space and resources against cells with a higher proliferative potential, the size of the cell population will ultimately grow again.

Whilst genetic mutations are a known source of phenotypic variability in cancer cell populations, a growing number of researchers welcome the contribution of epimutations (*i.e.* heritable phenotypic variations that are nongenetic in nature) in the events leading to the development and progression of cancer [13, 14, 21, 28, 33, 38, 44, 64, 68, 69, 77–79]. The initiation of genetic mutations is a result of abnormal structural changes in the DNA sequence, which incorporate a multitude of dissimilar alterations (*e.g.* replication error, neglected damage, substitution of base pairs and rearrangement). Epimutations, in contrast, act at the level of transcription by altering gene expression while leaving the order of the DNA bases unaltered. Gene expression may be upregulated, downregulated or even silenced, and the mechanisms through which this happens are of interest [30, 32]. DNA methylation and histone modification are two widely accepted epigenetic mechanisms in the development of resistance to chemotherapeutic agents, which both lead to gene silencing [60, 87].

The development of drugs which interfere with these epigenetic mechanisms and potentially revert cancerous cells back to a more normal phenotypic state appears to be a valuable resource for effective therapeutic protocols [66]. In this regard, a new perspective for cancer therapy is offered by experimental results showing that the so-called epigenetic drugs can induce the re-sensitisation of cancer cells to chemotherapeutic agents [1, 18, 49, 57, 74, 81, 89]. The role of epigenetic drugs is to interfere with the epigenetic machinery such that they promote re-expression of epigenetically regulated genes. Demethylating agents (which act to inhibit DNA methylation) and histone deacetylase (HDAC) inhibitors (which target the prevention of histone modification by acetylation) are two types of epigenetic drugs the effects of which prove promising on human

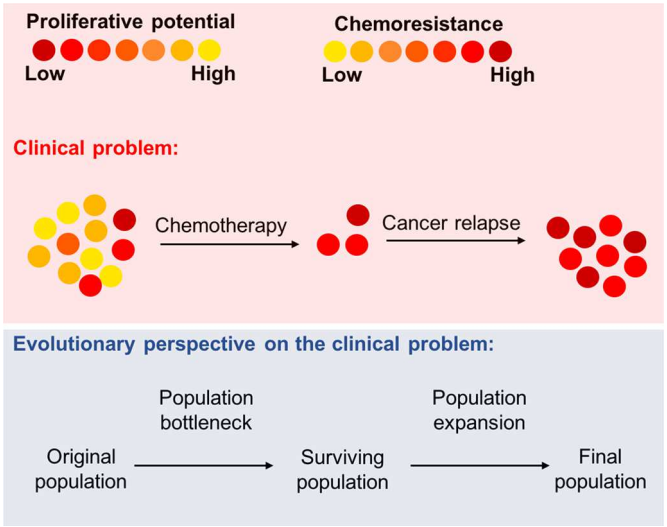

FIGURE 1. Schematic diagram illustrating the evolutionary process leading to the emergence of chemoresistance in cancer cell populations.

cancer. For instance, in melanoma and breast cancer studies, the methylation inhibitor 2-deoxy-5-azacytidine (DAC) demonstrated improved chemotherapeutic drug-uptake whilst reducing chemoresistance [41]. A mouse model showed no effect of DAC on tumour growth but revealed its ability to sensitise the tumour to other chemotherapeutic agents. Additionally, the HDAC inhibitor Vorinostat has the ability to sensitise cancer cells to other drug therapies; however, side effects prevent translation to the clinic [42]. Such drugs lie at the heart of controlling fundamental homeostatic mechanisms, rendering contrasting properties to those seen by chemotherapeutic drugs [89]. Researchers have discovered that inhibiting the DNA transcription regulator cyclin-dependent kinase 9 (CDK9) reactivates genes that have been epigenetically silenced by cancer, which leads to enhanced anti-cancer immunity [90]. Although the efficacy and side effects of this class of therapeutic agents are still largely to be assessed, within the past two decades seven epigenetic drugs have received regulatory approval, and numerous other candidates are currently in clinical trials [35].

2.2. A stochastic individual-based model for the phenotypic evolution of cancer cell populations

We study evolutionary dynamics of a well-mixed population of cancer cells structured by the expression level $y \in \mathbb{R}_{\geq 0}$ of an epigenetically regulated gene that controls both cell proliferation and chemoresistance, such as the DLL1 gene [47, 67, 72]. Cells within the population divide, die and undergo spontaneous epimutations, *i.e.* epimutations that occur randomly due to nongenetic instability and are not induced by any selective pressure [43]. Moreover, a chemotherapeutic agent can be administered as the primary treatment and an epigenetic drug promoting the re-expression of the gene may be used as an adjuvant treatment.

On the basis of previous experimental results, such as those reported in [37, 80], we follow Pisco and Huang [68] by assuming that there is a sufficiently high level of gene expression y^H conferring the highest rate of cellular division and, given that chemotherapeutic agents target mostly rapidly dividing cells [8], we also assume that there is a sufficiently low level of gene expression $y^L < y^H$ which endows cancer cells with the highest level of chemoresistance. Based on the modelling strategies proposed by Lorenzi *et al.* [52], we represent the phenotypic state of cancer cells by the rescaled variable $x \in \mathbb{R}$ with

$$x = \frac{y - y^L}{y^H - y^L},$$

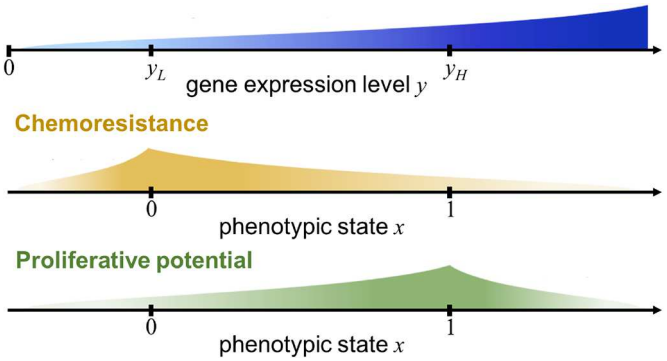

FIGURE 2. Schematic diagram illustrating the relationships between gene expression levels, phenotypic states and cellular characteristics in our model.

so that the state $x = 0$ corresponds to the highest level of chemoresistance, whereas the state $x = 1$ corresponds to the highest proliferative potential. These ideas are illustrated by the scheme in Figure 2.

Building upon the ideas presented by Chisholm *et al.* [23], we model the phenotypic evolution of the cell population as a time-discrete branching random walk whereby the time variable $t \in \mathbb{R}_{\geq 0}$ and the phenotypic state $x \in \mathbb{R}$ are discretised, respectively, as

$$t_h = h\tau \quad \text{for} \quad h \in \mathbb{N}_0 \quad \text{and} \quad x_i = i\chi \quad \text{for} \quad i \in \mathbb{Z}, \quad \text{with} \quad 0 < \tau, \chi \ll 1.$$

We introduce the dependent variable $N_i^h \in \mathbb{N}_0$ to model the number of cells in the phenotypic state x_i at the h^{th} time-step, and we compute the cell population density n_i^h, the size of the cell population (*i.e.* the total number of cells) ρ^h, the mean phenotypic state μ^h, and the related standard deviation σ^h as

$$n_i^h = N_i^h \, \chi^{-1}, \quad \rho^h = \sum_i N_i^h \quad \mu^h = \frac{1}{\rho^h} \sum_i x_i \, N_i^h \quad \text{and} \quad \sigma^h = \left(\frac{1}{\rho^h} \sum_i x_i^2 \, N_i^h - \left(\mu^h\right)^2 \right)^{\frac{1}{2}}. \tag{2.1}$$

Notice that the standard deviation σ^h provides a possible measure of the level of phenotypic heterogeneity within the cell population at the h^{th} time-step. Furthermore, focussing on the case of continuous drug administration, we introduce the parameters $c_{\mathrm{K}} \in [0, 1]$ and $c_{\mathrm{E}} \in [0, 1]$ to model, respectively, the rescaled constant concentration of the chemotherapeutic agent and of the epigenetic drug within the system.

We model the phenotypic evolution of the single cells by means of the following algorithmic rules, which are schematised in Figure 3.

Mathematical modelling of phenotypic variations (*cf.* Fig. 3(a)). To model the effect of spontaneous epimutations, at the beginning of each time-step h, we allow all cancer cells to update their phenotypic states according to a random walk. In summary, every cell in the population can undergo an epimutation and enter into a new phenotypic state with probability $\lambda \in [0, 1]$, or remain in its current phenotypic state with probability $1 - \lambda$. A cell in the phenotypic state x_i that undergoes an epimutation can either enter into the phenotypic state x_{i-1} with probability p_{L} or enter into the phenotypic state x_{i+1} with probability p_{R}. Hence, we assume that

$$p_{\mathrm{L}} + p_{\mathrm{R}} = \lambda. \tag{2.2}$$

Spontaneous epimutations are modulated by the epigenetic drug, which promotes the re-expression of the gene (*i.e.* it favours the transition of cancer cells from lower to higher values of x_i). We let the strength of the action

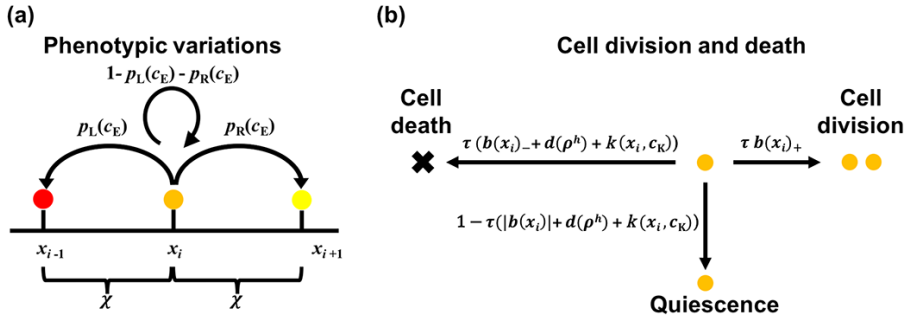

FIGURE 3. Schematic representation of the algorithmic rules governing the phenotypic evolution of cancer cells in the stochastic individual-based model. (a) Spontaneous epimutations are modelled as transitions between adjacent phenotypic states that occur with probabilities p_L and p_R. Epigenetic therapy is integrated into the model through the dependence of the transition probabilities on the concentration of the epigenetic drug c_E [*i.e.* $p_L \equiv p_L(c_E)$ and $p_R \equiv p_R(c_E)$]. (b) For a cell in the phenotypic state x_i, we let $b(x_i)$ and $k(x_i, c_K)$ model, respectively, the net rate of cell division (*i.e.* the difference between the rate of cell division and the rate of natural death) and the rate of cell death induced by the concentration c_K of the chemotherapeutic agent. Moreover, we denote by $d(\rho^h)$ the rate of cell death due to intrapopulation competition caused by nutrient and space limitations, with ρ^h being the size of the cell population at the time-step h. During the time interval of length $\tau \ll 1$ between the h^{th} time-step and the time-step $h+1$, we let a cell in the phenotypic state x_i divide with probability $\tau\, b(x_i)_+$ or die with probability $\tau\,\big(b(x_i)_- + d(\rho^h) + k(x_i, c_K)\big)$, or remain quiescent with probability $1 - \tau\,\big(|b(x_i)| + d(\rho^h) + k(x_i, c_K)\big)$.

of the epigenetic drug increase with the drug concentration; therefore, we make the assumptions that p_R is an increasing function of c_E. In more detail, we assume

$$p_L \equiv p_L(c_E), \quad p_R \equiv p_R(c_E), \quad p_R : [0,1] \to [0,\lambda], \quad p_R'(\cdot) \geq 0, \quad p_L(c_E) = \lambda - p_R(c_E), \tag{2.3}$$

and we choose

$$p_L(c_E) := \frac{\lambda}{2} - \frac{\nu}{2}\, c_E \quad \text{and} \quad p_R(c_E) := \frac{\lambda}{2} + \frac{\nu}{2}\, c_E, \tag{2.4}$$

where the parameter $\nu \in \mathbb{R}_{>0}$, with $\nu \ll 1$, models the strength of modulation of spontaneous epimutation by the epigenetic drug.

Mathematical modelling of cell division and death (*cf.* Fig. 3(b)). At any time-step h, after the phenotype update, we allow every cell to divide or die or remain quiescent at rates that depend on their phenotypic states, as well as on the environmental conditions given by the size of the cell population ρ^h and the concentration of the chemotherapeutic agent c_K. We denote by $b(x_i)$ the net division rate of a cell in the phenotypic state x_i (*i.e.* the difference between the rate of cell division and the rate of natural death). To take into account the fact that the phenotypic state $x = 1$ corresponds to the highest rate of cell division, we let the net cell division rate $b : \mathbb{R} \to \mathbb{R}$ satisfy following assumptions (see also Rem. 2.1)

$$b(1) > 0, \quad \arg\max_{x \in \mathbb{R}} b(x) = 1 \quad \text{and} \quad b''(\cdot) < 0. \tag{2.5}$$

Moreover, to translate into mathematical terms the idea that higher cell numbers correspond to less available space and resources, and thus to more intense intrapopulation competition, at every time-step h we allow the

cells to die due to intrapopulation competition at rate $d(\rho^h)$, where the function $d : \mathbb{R}_{\geq 0} \to \mathbb{R}_{\geq 0}$ satisfies the following assumptions

$$d(0) = 0 \quad \text{and} \quad d'(\cdot) > 0. \tag{2.6}$$

Finally, we denoted by $k(x_i, c_{\mathrm{K}})$ the rate at which a cell in the phenotypic state x_i can be induced to death by the chemotherapeutic agent. Since the cells in the phenotypic state $x = 0$ are fully chemoresistant and, for cells in phenotypic states other than the most chemoresistant one, the rate of death induced by chemotherapy increases with the dose of the chemotherapeutic agent, we assume the function $k : \mathbb{R} \times [0, 1] \to \mathbb{R}_{\geq 0}$ to satisfy the following conditions (see also Rem. 2.1)

$$k(\cdot, 0) = 0, \quad \arg\min_{x \in \mathbb{R}} k(x, c_K) = 0 \ \ \forall\, c_{\mathrm{K}} > 0, \quad \frac{\partial k(x, \cdot)}{\partial c_{\mathrm{K}}} > 0 \ \forall\, x \neq 0 \quad \text{and} \quad \frac{\partial^2 k(\cdot, c_{\mathrm{K}})}{\partial x^2} > 0 \ \ \forall\, c_{\mathrm{K}} > 0. \tag{2.7}$$

Remark 2.1. The concavity assumption on the net proliferation rate $b(x)$ and the convexity assumption on the rate of death induced by the chemotherapeutic agent $k(x, c_{\mathrm{K}})$ for $c_{\mathrm{K}} > 0$ lead naturally to smooth fitness landscapes (*cf.* Rem. 3.1), which are close to the approximate fitness landscapes inferred from experimental data through regression techniques [63].

In this framework, between the time-step h and the time-step $h + 1$, we let a cell in the phenotypic state x_i:

– divide (*i.e.* be replaced by two identical progeny cells) with probability

$$\tau\, b(x_i)_+ \quad \text{where} \quad b(x_i)_+ = \max\left(0, b(x_i)\right), \tag{2.8}$$

– die (*i.e.* be removed from the population) with probability

$$\tau \left(b(x_i)_- + d(\rho^h) + k(x_i, c_{\mathrm{K}}) \right) \quad \text{where} \quad b(x_i)_- = -\min\left(0, b(x_i)\right), \tag{2.9}$$

– remain quiescent with probability

$$1 - \tau \left(|b(x_i)| + d(\rho^h) + k(x_i, c_{\mathrm{K}}) \right) \quad \text{where} \quad |b(x_i)| = b(x_i)_+ + b(x_i)_-. \tag{2.10}$$

Notice that we assume the parameter τ to be sufficiently small so that the quantities (2.8)–(2.10) are all between 0 and 1.

On the basis of the ideas proposed in [23, 52], in this paper we will consider the following definitions

$$b(x) := \gamma - \eta\,(1 - x)^2, \quad d(\rho) := \zeta\, \rho, \quad k(x, c_{\mathrm{K}}) := c_{\mathrm{K}}\, x^2. \tag{2.11}$$

In the definitions (2.11), the parameter $\gamma \in \mathbb{R}_{>0}$ is the division rate of the fastest dividing cells in the phenotypic state $x = 1$, while the parameter $\eta \in \mathbb{R}_{>0}$ is a nonlinear selection gradient that provides a measure of the strength of natural selection in the absence of xenobiotic agents. Finally, the parameter $\zeta \in \mathbb{R}_{>0}$ is inversely proportional to the carrying capacity of the cancer cell population. The fact that the net proliferation rate $b(x)$ can become negative for values of x sufficiently far from 1 captures the idea that phenotypic variants with a low level of fitness cannot survive within the population. Definitions (2.11) satisfy assumptions (2.5)–(2.7) and ensure analytical tractability of the deterministic continuum counterpart of the stochastic discrete model, which will be formally derived in the next section.

3. Corresponding continuum model and analysis of evolutionary dynamics

3.1. Formal derivation of the continuum model corresponding to the individual-based model

Considering a cell population that evolves according to the algorithmic rules presented in Section 2.2 (*cf.* the scheme in Fig. 3), the principle of mass balance gives

$$n_i^{h+1} = \Big[2\tau b(x_i)_+ + 1 - \tau\big(\,|b(x_i)| + d(\rho^h) + k(x_i,c_{\mathrm{K}})\big)\Big]\Big[p_{\mathrm{L}}(c_{\mathrm{E}})\,n_{i+1}^h + p_{\mathrm{R}}(c_{\mathrm{E}})\,n_{i-1}^h + \big(1-p_{\mathrm{L}}(c_{\mathrm{E}})-p_{\mathrm{R}}(c_{\mathrm{E}})\big)n_i^h\Big].$$

Noting that

$$b(x_i) = b(x_i)_+ - b(x_i)_- \quad \text{and} \quad |b(x_i)| = b(x_i)_+ + b(x_i)_-,$$

the above difference equation can be rewritten as

$$n_i^{h+1} = \Big(1 + \tau\, b(x_i) - \tau\, d(\rho^h) - \tau\, k(x_i,c_{\mathrm{K}})\Big)\Big[p_{\mathrm{L}}(c_{\mathrm{E}})\,n_{i+1}^h + p_{\mathrm{R}}(c_{\mathrm{E}})\,n_{i-1}^h + \big(1-p_{\mathrm{L}}(c_{\mathrm{E}})-p_{\mathrm{R}}(c_{\mathrm{E}})\big)n_i^h\Big]. \tag{3.1}$$

Using the fact that the following relations hold for τ and χ sufficiently small

$$t_h \approx t, \quad t_{h+1} \approx t+\tau, \quad x_i \approx x, \quad x_{i-1} \approx x-\chi, \quad x_{i+1} \approx x+\chi,$$
$$n_i^h \approx n(x,t), \quad n_i^{h+1} \approx n(x,t+\tau), \quad n_{i-1}^h \approx n(x-\chi,t), \quad n_{i+1}^h \approx n(x+\chi,t), \quad \rho^h \approx \rho(t) = \int_{\mathbb{R}} n(x,t)\,\mathrm{d}x,$$

we rewrite (3.1) in the following approximate form

$$n(x,t+\tau) \approx \Big(1+\tau\,R(x,\rho(t),c_{\mathrm{K}})\Big)\Big[p_{\mathrm{L}}(c_{\mathrm{E}})\,n(x+\chi,t) + p_{\mathrm{R}}(c_{\mathrm{E}})\,n(x-\chi,t) + \big(1-p_{\mathrm{L}}(c_{\mathrm{E}})-p_{\mathrm{R}}(c_{\mathrm{E}})\big)n(x,t)\Big],$$

with

$$R(x,\rho,c_{\mathrm{K}}) := b(x) - d(\rho) - k(x,c_{\mathrm{K}}). \tag{3.2}$$

Assuming that $n \in C^2\left(\mathbb{R}\times\mathbb{R}_{\geq 0}\right)$, we can approximate the terms $n(x,t+\tau)$, $n(x-\chi,t)$ and $n(x+\chi,t)$ in the latter equation by their second order Taylor expansions about the point (x,t), that is, we can use the approximations

$$n(x,t+\tau) \approx n + \tau\frac{\partial n}{\partial t} + \frac{\tau^2}{2}\frac{\partial^2 n}{\partial t^2} \quad \text{and} \quad n(x\pm\chi,t) \approx n \pm \chi\frac{\partial n}{\partial x} + \frac{\chi^2}{2}\frac{\partial^2 n}{\partial x^2}, \quad \text{with} \quad n \equiv n(x,t).$$

In so doing, after a little algebra we find

$$\begin{aligned}\frac{\partial n}{\partial t} + \frac{\tau}{2}\frac{\partial^2 n}{\partial t^2} \approx{}& \frac{\chi}{\tau}\big(p_{\mathrm{L}}(c_{\mathrm{E}}) - p_{\mathrm{R}}(c_{\mathrm{E}})\big)\frac{\partial n}{\partial x} + \frac{\chi^2}{2\tau}\left(p_{\mathrm{L}}(c_{\mathrm{E}}) + p_{\mathrm{R}}(c_{\mathrm{E}})\right)\frac{\partial^2 n}{\partial x^2}\\ &+ R(x,\rho(t),c_{\mathrm{K}})\left[n + \chi\big(p_{\mathrm{L}}(c_{\mathrm{E}}) - p_{\mathrm{R}}(c_{\mathrm{E}})\big)\frac{\partial n}{\partial x} + \frac{\chi^2}{2}\big(p_{\mathrm{L}}(c_{\mathrm{E}}) + p_{\mathrm{R}}(c_{\mathrm{E}})\big)\frac{\partial^2 n}{\partial x^2}\right].\end{aligned} \tag{3.3}$$

Substituting (2.4) into (3.3) yields

$$\frac{\partial n}{\partial t}+\frac{\tau}{2}\frac{\partial^2 n}{\partial t^2}\approx-\frac{\chi\,\nu}{\tau}\,c_{\mathrm{E}}\frac{\partial n}{\partial x}+\frac{\chi^2}{\tau}\,\frac{\lambda}{2}\frac{\partial^2 n}{\partial x^2}+\,R(x,\rho(t),c_{\mathrm{K}})\left(n-\chi\,\nu\,c_{\mathrm{E}}\frac{\partial n}{\partial x}+\chi^2\frac{\lambda}{2}\frac{\partial^2 n}{\partial x^2}\right). \tag{3.4}$$

Letting $\nu,\tau,\chi\to 0$ in (3.4) in such a way that

$$\lim_{\nu,\tau,\chi\to 0}\frac{\chi\,\nu}{\tau}=\alpha\quad\text{and}\quad\lim_{\tau,\chi\to 0}\frac{\chi^2}{\tau}=\beta\quad\text{with}\quad\alpha,\beta\in\mathbb{R}_{>0} \tag{3.5}$$

we formally obtain the following nonlocal parabolic equation for the population density function $n(x,t)\geq 0$:

$$\begin{cases}\dfrac{\partial n}{\partial t}+\alpha\,c_{\mathrm{E}}\,\dfrac{\partial n}{\partial x}=\beta\,\dfrac{\lambda}{2}\,\dfrac{\partial^2 n}{\partial x^2}+R(x,\rho(t),c_{\mathrm{K}})\,n,\quad n\equiv n(x,t),\quad (x,t)\in\mathbb{R}\times\mathbb{R}_{\geq 0},\\[2ex]\rho(t)=\displaystyle\int_{\mathbb{R}}n(t,x)\,\mathrm{d}x.\end{cases} \tag{3.6}$$

Without loss of generality, in the remainder of this section we will assume

$$\alpha=\beta=1. \tag{3.7}$$

Remark 3.1. The functional $R(x,\rho,c_{\mathrm{K}})$ defined according to (3.2) represents the fitness of cancer cells in the phenotypic state x under the environmental conditions determined by the population size ρ and by the concentration of the chemotherapeutic agent c_{K}, *i.e.* the fitness landscape of the cancer cell population [43, 58, 70]. Substituting definitions (2.11) into definition (3.2), a little algebra shows that

$$R\big(x,\rho,c_{\mathrm{K}}\big)=\gamma-\frac{\eta\,c_{\mathrm{K}}}{\eta+c_{\mathrm{K}}}-(\eta+c_{\mathrm{K}})\left(x-\frac{\eta}{\eta+c_{\mathrm{K}}}\right)^2-\zeta\,\rho.$$

Therefore, the fittest phenotypic state (*i.e.* the phenotypic state with the highest fitness) is

$$x_{\mathrm{fit}}=\frac{\eta}{\eta+c_{\mathrm{K}}}$$

and the gene expression level corresponding to the fittest phenotypic state y_{fit} is given by the following equation

$$y_{\mathrm{fit}}=x_{\mathrm{fit}}\,y_H+(1-x_{\mathrm{fit}})\,y_L.$$

Hence, although $x\in\mathbb{R}$ and $y\in\mathbb{R}_{\geq 0}$, we have that

$$0<x_{\mathrm{fit}}\leq 1\quad\text{and}\quad y_L<y_{\mathrm{fit}}\leq y_H.$$

3.2. Analysis of evolutionary dynamics

For any initial condition $n(x,0)$ that satisfies the following biologically realistic assumptions

$$n(x,0)\in L^1\cap L^\infty(\mathbb{R}),\quad n(x,0)>0\text{ a.e. only on }\Omega\subset\mathbb{R}\text{ with }\Omega\text{ being a compact set,} \tag{3.8}$$

the long-time behaviour of the solution $n(x,t)\geq 0$ to equation (3.6) is characterised by Theorem 3.2.

Theorem 3.2. *Under definitions* (2.11) *and* (3.2) *and assumptions* (3.7)*, the integral* $\rho(t)$ *of the solution to the nonlocal parabolic PDE* (3.6) *subject to the initial condition* (3.8) *satisfies the following:*

(i) if

$$\frac{\eta\, c_{\mathrm{K}}}{\eta + c_{\mathrm{K}}} + \frac{c_{\mathrm{E}}^2}{2\,\lambda} + \left(\frac{\lambda}{2}\right)^{\frac{1}{2}} (\eta + c_{\mathrm{K}})^{\frac{1}{2}} \geq \gamma \tag{3.9}$$

then

$$\lim_{t\to\infty} \rho(t) = 0; \tag{3.10}$$

(ii) if

$$\frac{\eta\, c_{\mathrm{K}}}{\eta + c_{\mathrm{K}}} + \frac{c_{\mathrm{E}}^2}{2\,\lambda} + \left(\frac{\lambda}{2}\right)^{\frac{1}{2}} (\eta + c_{\mathrm{K}})^{\frac{1}{2}} < \gamma \tag{3.11}$$

then

$$\lim_{t\to\infty} \rho(t) = \overline{\rho} > 0 \quad \textit{with} \quad \overline{\rho} = \frac{1}{\zeta}\left(\gamma - \frac{\eta\, c_{\mathrm{K}}}{\eta + c_{\mathrm{K}}} - \frac{c_{\mathrm{E}}^2}{2\,\lambda} - \left(\frac{\lambda}{2}\right)^{\frac{1}{2}} (\eta + c_{\mathrm{K}})^{\frac{1}{2}}\right). \tag{3.12}$$

Moreover, under the additional assumption (3.11)*, the nonlocal parabolic PDE* (3.6) *admits a unique nonnegative nontrivial steady-state solution* $\overline{n}(x)$ *with*

$$\overline{n}(x) = \frac{\overline{\rho}}{(2\pi)^{\frac{1}{2}}\,\overline{\sigma}} \exp\left[-\frac{1}{2}\,\frac{(x-\overline{\mu})^2}{\overline{\sigma}^2}\right], \tag{3.13}$$

where

$$\overline{\mu} = \frac{\eta}{\eta + c_{\mathrm{K}}} + \frac{c_{\mathrm{E}}}{(2\,\lambda)^{\frac{1}{2}}\,(\eta + c_{\mathrm{K}})^{\frac{1}{2}}} \quad \textit{and} \quad \overline{\sigma} = \left(\frac{\lambda}{2\,(\eta + c_{\mathrm{K}})}\right)^{\frac{1}{4}}. \tag{3.14}$$

Proof. Substituting definitions (2.11) and (3.2) and assumptions (3.7) into the nonlocal parabolic PDE (3.6) gives

$$\frac{\partial n}{\partial t} + c_{\mathrm{E}}\,\frac{\partial n}{\partial x} = \frac{\lambda}{2}\,\frac{\partial^2 n}{\partial x^2} + \Big(\gamma - \eta\,(1-x)^2 - c_{\mathrm{K}}\,x^2 - \zeta\,\rho(t)\Big)n, \quad n \equiv n(x,t), \quad (x,t) \in \mathbb{R}\times\mathbb{R}_{\geq 0}.$$

We rewrite the latter PDE as

$$\frac{\partial n}{\partial t} + c_{\mathrm{E}}\,\frac{\partial n}{\partial x} = \frac{\lambda}{2}\,\frac{\partial^2 n}{\partial x^2} + \Big(\gamma_K - \eta_K\,(x - \overline{x}_K)^2 - \zeta\,\rho(t)\Big)n, \tag{3.15}$$

with

$$\gamma_K := \gamma - \frac{\eta\, c_{\mathrm{K}}}{\eta + c_{\mathrm{K}}}, \qquad \eta_K := \eta + c_{\mathrm{K}} \quad \text{and} \quad \overline{x}_K := \frac{\eta}{\eta + c_{\mathrm{K}}}. \tag{3.16}$$

Proof of (3.10) *and* (3.12). Using the method of proof that we presented in [23], one can show that, for any initial condition satisfying assumptions (3.8), the integral of the solution to the PDE (3.15) is such that

$$\rho(t) = \frac{\rho(0)\exp\left[\displaystyle\int_0^t g(s)\,\mathrm{d}s\right]}{1+\zeta\,\rho(0)\displaystyle\int_0^t \exp\left[\int_0^s g(z)\,\mathrm{d}z\right]\mathrm{d}s},$$

where the function $g(t)$ is such that $g(t) \longrightarrow \gamma_K - \dfrac{c_{\mathrm{E}}^2}{2\,\lambda} - \left(\dfrac{\lambda\,\eta_K}{2}\right)^{\frac{1}{2}} =: \overline{g}$ as $t \to \infty$. Since

$$\exp\left[\int_0^t g(s)\,\mathrm{d}s\right] \sim Ce^{\overline{g}\,t} \ \text{ as } t\to\infty \quad \text{and} \quad \int_0^t \exp\left[\int_0^s g(z)\,\mathrm{d}z\right]\mathrm{d}s \sim \begin{cases} const & \text{if } \overline{g}<0 \\ Ct & \text{if } \overline{g}=0 \\ \dfrac{C}{\overline{g}}e^{\overline{g}\,t} & \text{if } \overline{g}>0 \end{cases} \quad \text{as } t\to\infty$$

for some $C \in \mathbb{R}_{>0}$, we conclude that $\rho(t)$ is such that

$$\text{if } \gamma_K \le \frac{c_{\mathrm{E}}^2}{2\,\lambda} + \left(\frac{\lambda\,\eta_K}{2}\right)^{\frac{1}{2}} \ \text{ then } \ \lim_{t\to\infty}\rho(t) = 0, \ \text{ whereas if } \ \gamma_K > \frac{c_{\mathrm{E}}^2}{2\,\lambda} + \left(\frac{\lambda\,\eta_K}{2}\right)^{\frac{1}{2}} \ \text{ then } \ \lim_{t\to\infty}\rho(t) = \frac{\overline{g}}{\zeta}.$$

This concludes the proof of (3.10) and (3.12).

Proof of (3.13) *and* (3.14). A nonnegative nontrivial steady-state solution $\overline{n}(x)$ of the PDE (3.15) satisfies the following differential equation

$$\begin{cases} \dfrac{\lambda}{2}\,\overline{n}'' - c_{\mathrm{E}}\,\overline{n}' + \left(\gamma_K - \eta_K\,(x-\overline{x}_K)^2 - \zeta\,\overline{\rho}\right)\overline{n} = 0, \quad \overline{n}\equiv\overline{n}(x), \quad x\in\mathbb{R}, \\ \overline{\rho} = \displaystyle\int_{\mathbb{R}} \overline{n}(x)\,\mathrm{d}x. \end{cases} \tag{3.17}$$

We make the change of variables $y = x - \overline{x}_K$ and rewrite (3.17) as

$$\begin{cases} \dfrac{\lambda}{2}\,\overline{n}'' - c_{\mathrm{E}}\,\overline{n}' + \left(\gamma_K - \eta_K\,y^2 - \zeta\,\overline{\rho}\right)\overline{n} = 0, \quad \overline{n}\equiv\overline{n}(y), \quad y\in\mathbb{R}, \\ \overline{\rho} = \displaystyle\int_{\mathbb{R}} \overline{n}(y)\,\mathrm{d}y. \end{cases} \tag{3.18}$$

Making the additional change of variables

$$\overline{n}(y) = \exp\left(\frac{c_{\mathrm{E}}\,y}{\lambda}\right)u(z) \quad \text{with} \quad z = y\left(\frac{8\,\eta_K}{\lambda}\right)^{\frac{1}{4}} \tag{3.19}$$

we find that $u(z)$ satisfies the differential equation

$$u'' - \left(\frac{z^2}{4} + a\right) u = 0, \quad u \equiv u(z), \quad z \in \mathbb{R} \quad \text{with} \quad a := \frac{\zeta}{(2\,\lambda\,\eta_K)^{\frac{1}{2}}} \left(\overline{\rho} + \frac{c_{\mathrm{E}}^2}{2\,\lambda\,\zeta} - \frac{\gamma_K}{\zeta}\right). \tag{3.20}$$

The differential equation (3.20) is the Weber's equation, the solutions of which are bounded for all $z \in \mathbb{R}$ if and only if

$$a = -m - \frac{1}{2} \quad \text{with} \quad m \in \mathbb{Z}^*.$$

The bounded solutions are of the form

$$u(z) \propto \exp(-z^2/4)\, \mathcal{H}_m(z), \tag{3.21}$$

where $\mathcal{H}_m(z)$ denotes the Hermite polynomial of degree m [59, 84]. Since $\mathcal{H}_m(z) \geq 0$ for all $z \in \mathbb{R}$ only if $m = 0$, the existence of a nontrivial nonnegative solution of the differential equation (3.20) requires $a = -\frac{1}{2}$. Under assumption (3.11), solving the algebraic equation

$$a = -\frac{1}{2} \iff \frac{\zeta}{(2\,\lambda\,\eta_K)^{\frac{1}{2}}} \left(\overline{\rho} + \frac{c_{\mathrm{E}}^2}{2\,\lambda\,\zeta} - \frac{\gamma_K}{\zeta}\right) = -\frac{1}{2}$$

for $\overline{\rho}$ we find the expression (3.12) of $\overline{\rho}$, as expected. Furthermore, using equation (3.21) with $m = 0$ along with the change of variables (3.19) we find that

$$\overline{n}(y) = C \exp\left[-\frac{1}{2}\left(\frac{2\,\eta_K}{\lambda}\right)^{\frac{1}{2}} \left(y - \frac{c_{\mathrm{E}}}{(2\,\lambda\,\eta_K)^{\frac{1}{2}}}\right)^2\right],$$

for some $C \in \mathbb{R}_{>0}$. The change of variables $y = x - \overline{x}_K$ then yields

$$\overline{n}(x) = C \exp\left\{-\frac{1}{2}\left(\frac{2\,\eta_K}{\lambda}\right)^{\frac{1}{2}} \left[x - \left(\overline{x}_K + \frac{c_{\mathrm{E}}}{(2\,\lambda\,\eta_K)^{\frac{1}{2}}}\right)\right]^2\right\}. \tag{3.22}$$

Moreover, we can evaluate the constant C in terms of $\overline{\rho}$ by integrating both sides of (3.22) over $\mathbb{R}$ and imposing $\int_{\mathbb{R}} \overline{n}(x)\, \mathrm{d}x = \overline{\rho}$. In so doing we find $C = \overline{\rho}\, (2\pi)^{-\frac{1}{2}} \left(\frac{\lambda}{2\,\eta_K}\right)^{-\frac{1}{4}}$. Substituting the expression of C together with the definitions (3.16) of η_K and $\overline{x}_K$ into (3.22) we obtain (3.13) with $\overline{\mu}$ and $\overline{\sigma}$ given by (3.14). This concludes the proof of (3.13) and (3.14). □

Additional pieces of biological information are conveyed by the result established by the following corollary of Theorem 3.2.

Corollary 3.3. *Under the assumptions of Theorem 3.2 and the additional assumption* (3.11)*, if the following condition is verified*

$$c_{\mathrm{E}} > \lambda^{\frac{3}{4}} \left(\frac{\eta + c_{\mathrm{K}}}{2}\right)^{\frac{1}{4}} \tag{3.23}$$

then the asymptotic value of the cell population size (3.12) *is such that*

$$\frac{\partial \overline{\rho}}{\partial \lambda} > 0. \tag{3.24}$$

Proof. Differentiating the expression (3.12) of $\overline{\rho}$ with respect to λ and solving the inequality $\dfrac{\partial \overline{\rho}}{\partial \lambda} > 0$ for c_{E} one can easily verify the claim of Corollary 3.3. □

The asymptotic results established by Theorem 3.2 together with the additional result given by Corollary 3.3 demonstrate that, if the cancer cell population does not go extinct, *i.e.* if assumption (3.11) is satisfied, then:

- The equilibrium population size $\overline{\rho}$ is a decreasing function of the concentration of the chemotherapeutic agent c_{K} and of the concentration of the epigenetic drug c_{E}.
- The reduction in the equilibrium population size induced by the chemotherapeutic agent is an increasing function of the selection gradient η and of the probability of spontaneous epimutation λ.
- The reduction in the equilibrium population size due to the epigenetic drug is a decreasing function of the probability of spontaneous epimutation λ.
- If the concentration of the epigenetic drug is sufficiently high – *i.e.* when c_{E} satisfies condition (3.23) – the population size at equilibrium is an increasing function of λ.
- The equilibrium phenotype distribution $\overline{n}(x)$ is unimodal, with the mean phenotypic state $\overline{\mu}$ being at the distribution's peak.
- If $c_{\mathrm{E}} = 0$ and $c_{\mathrm{K}} = 0$ then $\overline{\mu} = 1$, that is, in the absence of xenobiotic agents the peak of the equilibrium phenotype distribution is at the fastest proliferating state $x = 1$.
- The mean phenotypic state $\overline{\mu}$ is a decreasing function of the concentration of the chemotherapeutic agent c_{K}. Higher values of c_{K} lead the peak of the equilibrium phenotype distribution to move from the fastest proliferating state $x = 1$ towards more chemoresistant phenotypic states closer to the most chemoresistant state $x = 0$.
- The level of phenotypic heterogeneity at equilibrium (*i.e.* the standard deviation $\overline{\sigma}$ of the phenotypic distribution) is an increasing function of the probability of spontaneous epimutation λ, and a decreasing function of both the nonlinear selection gradient η and the concentration of the chemotherapeutic agent c_{K}.
- The mean phenotypic state $\overline{\mu}$ is an increasing function of the concentration of the epigenetic drug c_{E}. For $c_{\mathrm{K}} > 0$ given, higher values of c_{E} move the peak of the equilibrium phenotype distribution from more chemoresistant phenotypic states closer to $x = 0$ towards more chemosensitive phenotypic states closer to $x = 1$.
- For $c_{\mathrm{E}} > 0$ given, the change in the mean phenotypic state $\overline{\mu}$ induced by the epigenetic drug is a decreasing function of the probability of spontaneous epimutation λ and of the concentration of the chemotherapeutic agent c_{K}.

In the next section, these mathematical findings are integrated with the results of computational simulations of the stochastic individual-based model, and their biological relevance is discussed in detail.

4. Computational simulations of the stochastic individual-based model

4.1. Setup of computational simulations

To carry out computational simulations of the stochastic individual-based model, we consider $x \in [-4, 4] \subset \mathbb{R}$ and we define $\tau = 0.001$, $\chi = \sqrt{\tau}$ and $\nu = \chi$, so that conditions (3.5) and (3.7) are met. In agreement with previous papers [11, 12, 52, 69, 82], we define

$$\gamma := 0.6 \text{ day}^{-1}, \quad \eta := 0.3 \text{ day}^{-1}, \quad \zeta := 0.6 \times 10^{-4} \text{ cells}^{-1} \text{ day}^{-1} \tag{4.1}$$

and, unless otherwise stated, we choose

$$\lambda := 0.01. \tag{4.2}$$

Computational simulations are carried out in MATLAB. At each time-step, we follow the procedures summarised hereafter to simulate phenotypic variations, cell division and cell death. All random numbers mentioned below are real numbers drawn from the standard uniform distribution on the interval $(0, 1)$ using the MATLAB function RAND.

- *Phenotypic variations.* For each cell, a random number is generated and we determine whether or not the cell undergoes a phenotypic variation by comparing this number with the value of the probability of epimutation λ. If a cell undergoes a phenotypic variation, a new random number is generated and we let the cell move either into the phenotypic state to the left or into the phenotypic state to the right of its current state based on a comparison between the random number and the values of the quantities $p_L(c_E)$ and $p_R(c_E)$ defined according to (2.4). The attempted phenotypic variation of the cell is aborted if it requires moving out of the computational domain $[-4, 4]$.

- *Cell division and death.* The size of the cell population is computed and the probabilities of cell division, death and quiescence are evaluated for every phenotypic state according to (2.8)–(2.11). For each cell, a random number is generated and the cells' fate is determined by comparing this number with the probabilities of division, death and quiescence corresponding to the cell phenotypic state.

We study the evolution of the cell population over the time window $[0, T]$ with T corresponding to 60 days. The average CPU time for one computational simulation is 62 seconds.

To reproduce a biological scenario where the cell population has never been exposed to therapy, we consider an initial cell number approximatively equal to the equilibrium population size (3.12) for $c_{\mathrm{E}} = 0$ and $c_{\mathrm{K}} = 0$ (*i.e.* the initial total number of cells is 8841). Moreover, we assume the phenotypic states of the cells to be initially distributed according to a normal distribution with mean zero (*i.e.* most of the cells are initially in the fastest dividing state $x = 0$).

For all the computational simulations of the individual-based model that we report on in this section, we show that the size of the cell population ρ^h, the mean phenotypic state μ^h and the population density n_i^h at day 60 match, respectively, with the equilibrium population size $\overline{\rho}$, the equilibrium average phenotypic state $\overline{\mu}$, and the equilibrium population density $\overline{n}(x)$ given by (3.12)–(3.14). This testifies to the robustness of the computational results presented here.

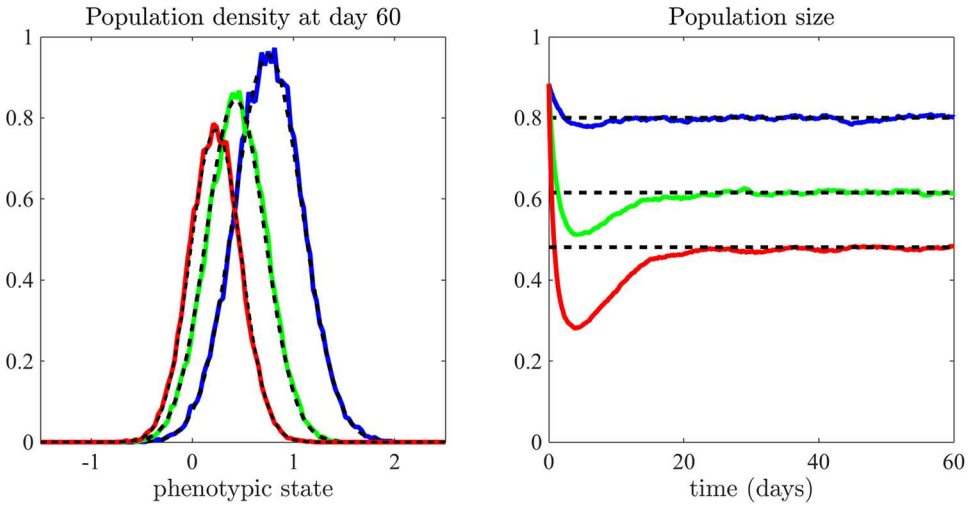

FIGURE 4. Population density n_i^h at day 60 and corresponding dynamics of the population size ρ^h for increasing concentrations of the chemotherapeutic agent – *i.e.* $c_{\mathrm{K}} = 0.1$ (*blue lines*), $c_{\mathrm{K}} = 0.4$ (*green lines*) and $c_{\mathrm{K}} = 1$ (*red lines*) – in the absence of the epigenetic drug – *i.e.* $c_{\mathrm{E}} = 0$. The black dashed lines highlight the equilibrium population density $\overline{n}(x)$ and the equilibrium population size $\overline{\rho}$ given by (3.13) and (3.12), respectively. Values are in units of 10^4.

4.2. Main results

The chemotherapeutic agent reduces the population size at the cost of promoting the outgrowth of more chemoresistant phenotypic variants

The computational simulation results presented in Figure 4 show that, in the absence of epigenetic therapy (*i.e.* when $c_{\mathrm{E}} = 0$), higher doses of the chemotherapeutic agent (*i.e.* higher values of c_{K}) trigger a more pronounced population bottleneck by causing a sharper reduction in the total number of cells before re-growth towards a stable value. The black dashed lines in Figure 4 highlight the equilibrium population size $\overline{\rho}$ (*right panel*) and the equilibrium population density $\overline{n}(x)$ (*left panel*) given, respectively, by (3.12) and (3.13). In agreement with the asymptotic results established by Theorem 3.2, the population density at day 60 is unimodal with the distribution's peak being closer to the highly-chemoresistant phenotypic state $x = 0$ for higher values of c_{K}, while the corresponding population size is a decreasing function of the dose of the chemotherapeutic agent. These results formalise the idea that chemotherapy reduces the size of cancer cell populations at the cost of promoting the selection of more chemoresistant phenotypic variants.

The level of phenotypic heterogeneity in the population decreases with the concentration of the chemotherapeutic agent

The computational simulation results presented in the right panel of Figure 4 reveal also that the standard deviation of the population density n_i^h at day 60 decreases with the concentration of the chemotherapeutic agent. This is in agreement with the asymptotic results established by Theorem 3.2, and reflects the fact that chemotherapy acts as a selective pressure on cancer cells, thus reducing the level of phenotypic heterogeneity within the population.

Higher probabilities of spontaneous epimutation and larger selection gradients increase the cytotoxic effect of the chemotherapeutic agent

The heat map in the left panel of Figure 5 depicts how the population size ρ^h at day 60 varies as a function of the probability of spontaneous epimutation λ and of the nonlinear selection gradient η, under chemotherapy

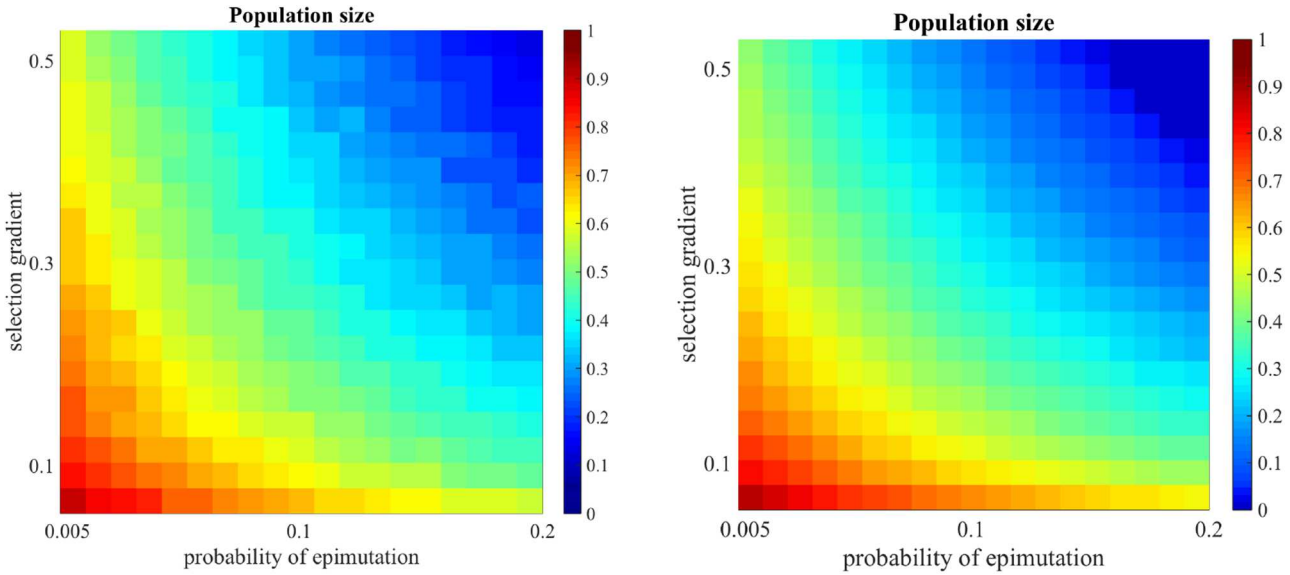

FIGURE 5. The plot in the left panel shows the population size ρ^h (in units of 10^4) at day 60 as a function of the probability of spontaneous epimutation λ and of the selection gradient η. The concentration of the chemotherapeutic agent is $c_K = 0.5$ and there is no epigenetic drug (*i.e.* $c_E = 0$). This plot matches with the plot of the equilibrium population size $\overline{\rho}$ given by (3.12) as a function of the parameters λ and η, which is displayed in the right panel.

as a stand alone treatment (*i.e.* for $c_K > 0$ and $c_E = 0$). The plot matches with the same plot of the equilibrium population size $\overline{\rho}$ given by (3.12), which is displayed in the right panel of Figure 5. These results indicate that, in the absence of epigenetic therapy, the cell population size at day 60 is a decreasing function of the parameters λ and η, which supports the idea that the cytotoxic effect of the chemotherapeutic agent becomes stronger in the presence of higher probabilities of spontaneous epimutation and larger selection gradients.

The epigenetic drug reduces the size of the population and counters the selection of chemoresistant phenotypic variants

The results presented in Figure 6 summarise the effects on the cell population of adjuvant epigenetic therapy. The black dashed lines highlight the equilibrium population density $\overline{n}(x)$ (*left panel*) and the equilibrium population size $\overline{\rho}$ (*right panel*) given by (3.13) and (3.12), respectively. In agreement with the asymptotic results established by Theorem 3.2, the computational simulation results displayed in the insets in the right panel of Figure 6 show that, for all the doses of the chemotherapeutic agent considered here (*i.e.* all values of $c_K > 0$ used to carry out computational simulations), the population size ρ^h at day 60 is lower under adjuvant epigenetic therapy (*i.e.* when $c_E > 0$) compared to the case without epigenetic drug (*i.e.* for $c_E = 0$). Furthermore, the cell population density n_i^h at day 60 is unimodal, and the phenotype distribution's peak for $c_E > 0$ is further away from the highly-chemoresistant phenotypic state $x = 0$ than in the case where $c_E = 0$ (*vid.* insets in the left panel of Figure 6). The distance between the values of the mean phenotypic state μ^h at day 60 obtained for $c_E > 0$ and $c_E = 0$ is a decreasing function of c_K. Taken together, these results support the idea that combining primary chemotherapy with adjuvant epigenetic therapy makes it possible to induce to death a larger number of cancer cells, and meanwhile hamper the selection of chemoresistant phenotypic variants. Moreover, the results predict that epigenetic drugs promoting the re-expression of epigenetically regulated genes will be more effective in preventing the emergence of chemoresistance under low-dose chemotherapy than under high-dose chemotherapy.

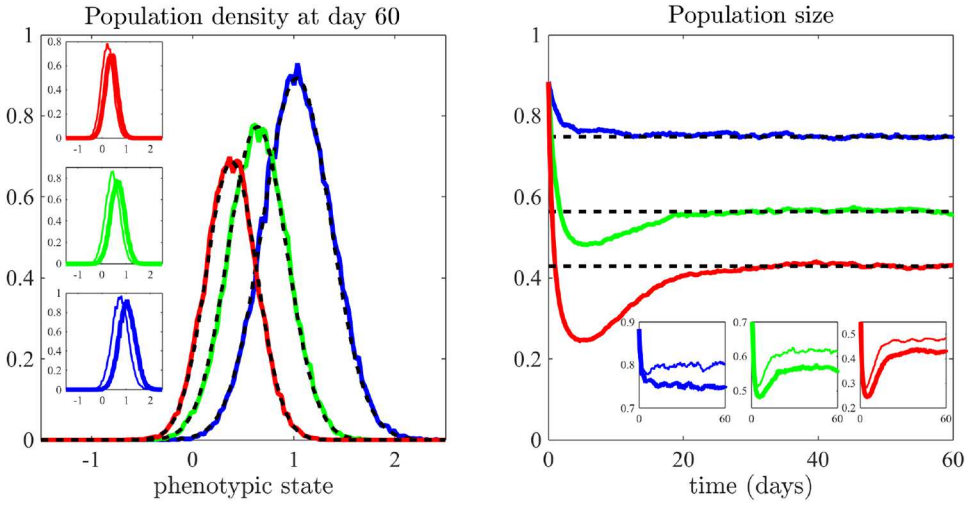

FIGURE 6. Population density n_i^h at day 60 and corresponding dynamics of the population size ρ^h for increasing concentrations of the chemotherapeutic agent – *i.e.* $c_K = 0.1$ (*blue lines*), $c_K = 0.4$ (*green lines*) and $c_K = 1$ (*red lines*) – in the presence of the epigenetic drug – *i.e.* $c_E = 0.025$. The black dashed lines highlight the equilibrium population density $\overline{n}(x)$ and the equilibrium population size $\overline{\rho}$ given by (3.13) and (3.12), respectively. The insets show the comparison between the results obtained with (ticker lines) and without (*thiner lines*) the epigenetic drug (*i.e.* for $c_E > 0$ and $c_E = 0$, respectively). Values are in units of 10^4.

The action of the epigenetic drug is hampered by higher probabilities of spontaneous epimutation

The results presented in Figure 7 illustrate how the size ρ^h and the mean phenotypic state μ^h of the cell population at day 60 vary as functions of the probability of spontaneous epimutation λ under chemotherapy (*i.e.* for $c_K > 0$). Different colours correspond to different doses of the epigenetic drug (*i.e.* different values of c_E). The dashed lines highlight the equilibrium population size $\overline{\rho}$ and the equilibrium mean phenotypic state $\overline{\mu}$ given by (3.12) and (3.14), respectively, as functions of the parameter λ. In agreement with the asymptotic results established by Theorem 3.2, the mean phenotypic state μ^h at day 60 does not depend on the probability of spontaneous epimutation under chemotherapy as a stand-alone treatment (*i.e.* for $c_K > 0$ and $c_E = 0$), while it becomes a decreasing function of the parameter λ in the presence of adjuvant epigenetic therapy (*i.e.* when $c_K > 0$ and $c_E > 0$). This suggests that epigenetic drugs can become less effective in countering the emergence of chemoresistance in those cases where cancer cells are more likely to undergo spontaneous epimutations.

The epigenetic drug can alter dependence of the cell population size on the probability of spontaneous epimutation

The computational simulation results presented in Figure 7 also show that, in the absence of the epigenetic drug, the cell population size ρ^h at day 60 is a decreasing function of the probability of spontaneous epimutation λ. On the other hand, as established by Corollary 3.3, if the dose of the epigenetic drug is sufficiently high [*i.e.* if condition (3.23) is verified] then the cell population size ρ^h at day 60 is an increasing function of λ. This communicates the notion that epigenetic drugs which induce gene re-expression may alter the existing relationships between the probability of spontaneous epimutation and the size of cancer cell populations.

Considerations about therapeutic optimisation

The plots in Figure 8 illustrate how the size ρ^h and the mean phenotypic state μ^h of the cell population at day 60 vary as functions of the total concentration of the therapeutic agents (*i.e.* different values of the sum $c_K + c_E$).

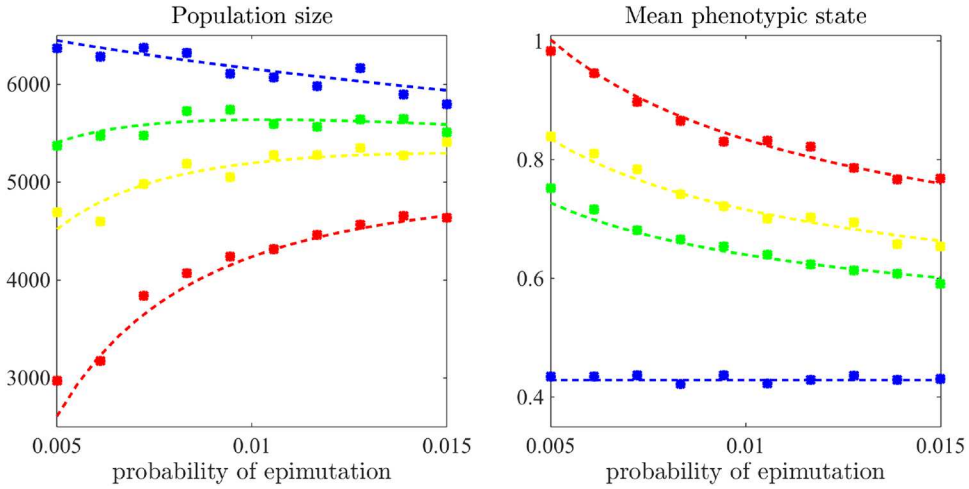

FIGURE 7. Plots of the population size ρ^h and the mean phenotypic state μ^h at day 60 as functions of the probability of spontaneous epimutation λ. The concentration of the chemotherapeutic agent is $c_K = 0.4$, while the concentration of the epigenetic drug is alternatively defined as $c_E = 0$ (*blue dots*), $c_E = 0.025$ (*green dots*), $c_E = 0.034$ (*yellow dots*) or $c_E = 0.048$ (*red dots*). The values of c_E corresponding to the yellow and *red lines* are such that the condition (3.23) is satisfied for all values of λ considered. The dashed lines highlight the equilibrium population size $\overline{\rho}$ and the equilibrium mean phenotypic state $\overline{\mu}$ given by (3.12) and (3.14), respectively.

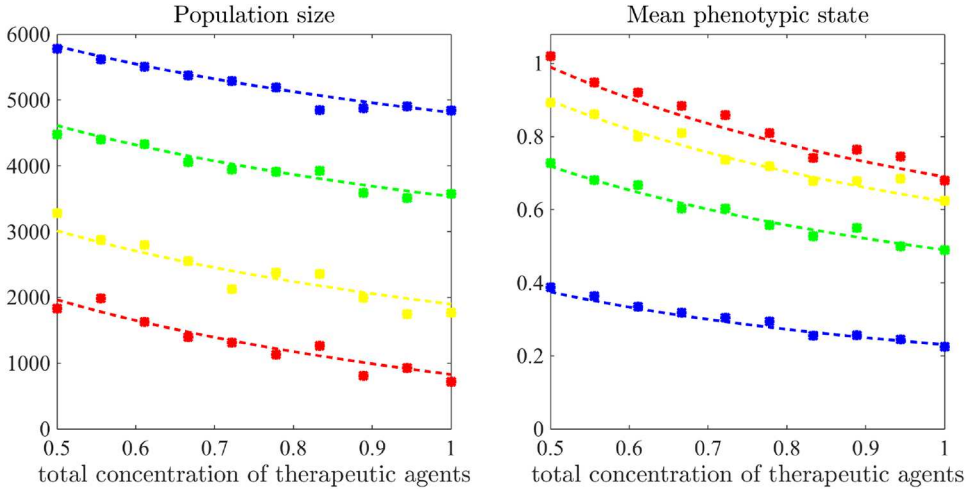

FIGURE 8. Plots of the population size ρ^h and the average phenotypic state μ^h at day 60 as functions of the total concentration of therapeutic agents $c_E + c_K$, *i.e.* $c_K \in [0.5 - c_E, 1 - c_E]$ with $c_E = 0$ (*blue dots*), $c_E = 0.04$ (*green dots*), $c_E = 0.06$ (*yellow dots*) and $c_E = 0.07$ (*red dots*). The dashed lines highlight the equilibrium population size $\overline{\rho}$ and the equilibrium mean phenotypic state $\overline{\mu}$ given by (3.12) and (3.14), respectively.

Different colours correspond to different combinations of the chemotherapeutic agent and the epigenetic drug (*i.e.* different values of $c_K > 0$ and $c_E \geq 0$ that give the same value of $c_K + c_E$). The dashed lines highlight the corresponding values of the equilibrium population size $\overline{\rho}$ and the equilibrium mean phenotypic state $\overline{\mu}$ given by (3.12) and (3.14), respectively. These results show that, for each given value of the total concentration of

therapeutic agents, values of the mean phenotypic state more distant from the highly-chemoresistant phenotypic state $x = 0$ and lower values of the size of the cell population can be obtained by increasing the value of c_{E} and decreasing the value of c_{K}. This supports the conclusion that therapeutic protocols based on lower doses of chemotherapeutic agents in combination with epigenetic drugs that promote the re-expression of epigenetically regulated genes can lead to a better therapeutic outcome – a therapeutic outcome characterised by smaller cancer cell numbers and lower levels of chemoresistance – than therapeutic protocols based solely on high-dose chemotherapy.

5. Conclusions and research perspectives

We have developed a simple, yet effective, phenotype-structured individual-based model for the evolution of a cancer cell population under the action of a chemotherapeutic agent in combination with an epigenetic drug. Moreover, we have formally derived the deterministic continuum counterpart of such a stochastic discrete model, which is given by a nonlocal PDE for the population density function. Integrating the results of computational simulations of the stochastic individual-based model with analytical results on the long-term behaviour of the solution to the corresponding PDE, we have obtained findings with broad structural stability under parameter changes. The results achieved give answers to questions **Q1**–**Q4** posed in Section 2. In summary:

- **A1** Our results support the idea that chemotherapeutic agents reduce the size of cancer cell populations at the cost of promoting the outgrowth of more resistant phenotypic variants. Moreover, the level of chemoresistance acquired by cancer cell populations can vary with the administered dose of the chemotherapeutic agent. This suggests that different doses of the same agent can trigger the selection for phenotypic variants characterised by different levels of chemoresistance. Finally, the results presented here indicate that the level of phenotypic heterogeneity in cancer cell populations decreases with the concentration of chemotherapeutic agents, which reflects the fact that higher doses of chemotherapy correspond to harsher environmental conditions and stronger selective pressures.
- **A2** The results of this *in silico* study suggest that, under the continuous administration of chemotherapeutic agents, harsher environmental conditions (*i.e.* stronger selection gradients independent of xenobiotic agents) and higher probabilities of spontaneous epimutation can make cancer cell populations more sensitive to the cytotoxic action of chemotherapy.
- **A3** Our results demonstrate the existence of an inverse relationship between the efficacy of epigenetic drugs and the probability for cancer cells to undergo spontaneous epimutations. Furthermore, the model supports the idea that epigenetic drugs can be more effective in countering the emergence of chemoresistance when used in combination with low-dose chemotherapy.
- **A4** The outcomes of the model provide theoretical ground for the development of anticancer protocols that use lower concentrations of chemotherapeutic agents in combination with epigenetic drugs capable of promoting the re-expression of epigenetically regulated genes; with the caveat that such drugs may alter the way in which spontaneous epimutations impact on the evolution of cancer cell populations.

The focus of this work has been on the case of continuous drug administration. However, the stochastic individual-based model presented here, as well as the related formal method to derive the corresponding deterministic continuum model, can be easily adapted to drug doses that vary over time. In this regard, it would be interesting to investigate whether the delivery schedules for the chemotherapeutic agent obtained through numerical optimal control of the nonlocal PDE for the population density function [2, 62] would remain optimal also for the individual-based model. Another track to follow might be to investigate the effect of stress-induced epimutations triggered by the selective pressure that chemotherapeutic agents exert on cancer cells [25]. An additional development of this study would be to include a spatial structure, for instance by embedding the cancer cells in the geometry of a solid tumour, and to take explicitly into account the effect of spatial interactions between cancer cells, therapeutic agents and other abiotic factors, such as oxygen and glucose [54, 55]. In this case, the resulting individual-based model would be integrated with a system of PDEs modelling the dynamics

of the abiotic factors, thus leading to a hybrid model [4, 9, 10, 15, 16, 31, 34, 40, 48, 75, 76]. These are all lines of research that we will be pursuing in the near future.

References

[1] N. Ahuja, A.R. Sharma and S.B. Baylin, Epigenetic therapeutics: a new weapon in the war against cancer. *Annu. Rev. Med.* **67** (2016) 73–89.

[2] L. Almeida, P. Bagnerini, G. Fabrini, B.D. Hughes and T. Lorenzi, Evolution of cancer cell populations under cytotoxic therapy and treatment optimisation: insight from a phenotype-structured model. *ESAIM: M2AN* **53** (2019) 1157–1190.

[3] P.M. Altrock, L.L. Liu and F. Michor, The mathematics of cancer: integrating quantitative models. *Nat. Rev. Cancer* **15** (2015) 730.

[4] A.R. Anderson and M. Chaplain, Continuous and discrete mathematical models of tumor-induced angiogenesis. *Bull. Math. Biol.* **60** (1998) 857–899.

[5] A.R. Anderson and V. Quaranta, Integrative mathematical oncology. *Nat. Rev. Cancer* **8** (2008) 227.

[6] A.R.A. Anderson and P.K. Maini, Mathematical oncology. *Bull. Math. Biol.* **80** (2018) 945–953.

[7] N. Beerenwinkel, C.D. Greenman and J. Lagergren, Computational cancer biology: an evolutionary perspective. *PLOS Comput. Biol.* **12** (2016) e1004717.

[8] M.V. Blagosklonny, Target for cancer therapy: proliferating cells or stem cells. *Leukemia* **20** (2006) 385–391.

[9] A. Bouchnita, F.-E. Belmaati, R. Aboulaich, M. Koury and V. Volpert, A hybrid computation model to describe the progression of multiple myeloma and its intra-clonal heterogeneity. *Computation* **5** (2017) 16.

[10] A. Bouchnita, N. Eymard, T.K. Moyo, M.J. Koury and V. Volpert, Bone marrow infiltration by multiple myeloma causes anemia by reversible disruption of erythropoiesis. *Am. J. Hematol.* **91** (2016) 371–378.

[11] I. Bozic, B. Allen and M. A. Nowak, Dynamics of targeted cancer therapy. *Trends Mol. Med.* **18** (2012) 311–316.

[12] I. Bozic, J.G. Reiter, B. Allen, T. Antal, K. Chatterjee, P. Shah, Y.S. Moon, A. Yaqubie, N. Kelly, D.T. Le, *et al.*, Evolutionary dynamics of cancer in response to targeted combination therapy. *Elife* **2** (2013) e00747.

[13] A. Brock, H. Chang and S. Huang, Non-genetic heterogeneity—a mutation-independent driving force for the somatic evolution of tumours, *Nat. Rev. Genet.* **10** (2009) 336–342.

[14] R. Brown, E. Curry, L. Magnani, C. S. Wilhelm-Benartzi and J. Borley, Poised epigenetic states and acquired drug resistance in cancer. *Nat. Rev. Cancer* **14** (2014) 747.

[15] A.E. Burgess, T. Lorenzi, P.G. Schofield, S.F. Hubbard and M.A. Chaplain, Examining the role of individual movement in promoting coexistence in a spatially explicit prisoner's dilemma. *J. Theor. Biol.* **419** (2017) 323–332.

[16] A.E. Burgess, P.G. Schofield, S.F. Hubbard, M.A. Chaplain, and T. Lorenzi, Dynamical patterns of coexisting strategies in a hybrid discrete-continuum spatial evolutionary game model. *MMNP* **11** (2016) 49–64.

[17] H.M. Byrne, Dissecting cancer through mathematics: from the cell to the animal model. *Nat. Rev. Cancer* **10** (2010) 221–230.

[18] K. Camphausen and P.J. Tofilon, Inhibition of histone deacetylation: a strategy for tumor radiosensitization. *J. Clin. Oncol.* **25** (2007) 4051–4056.

[19] N. Champagnat, R. Ferrière and G. Ben Arous, The canonical equation of adaptive dynamics: a mathematical view. *Selection* **2** (2002) 73–83.

[20] N. Champagnat, R. Ferrière and S. Méléard, Unifying evolutionary dynamics: from individual stochastic processes to macroscopic models. *Theor. Populat. Biol.* **69** (2006) 297–321.

[21] W. Chen, T.K. Cooper, C.A. Zahnow, M. Overholtzer, Z. Zhao, M. Ladanyi, J.E. Karp, N. Gokgoz, J.S. Wunder, I.L. Andrulis, A.J. Levine, J.L. Mankowski and S.B. Baylin, Epigenetic and genetic loss of hic1 function accentuates the role of p53 in tumorigenesis. *Cancer Cell* **6** (2004) 387–398.

[22] R.H. Chisholm, T. Lorenzi and J. Clairambault, Cell population heterogeneity and evolution towards drug resistance in cancer: biological and mathematical assessment, theoretical treatment optimisation. *Biochim. Biophys. Acta* **1860** (2016) 2627–2645.

[23] R.H. Chisholm, T. Lorenzi, L. Desvillettes and B.D. Hughes, Evolutionary dynamics of phenotype-structured populations: from individual-level mechanisms to population-level consequences. *Z. Angew. Math. Phys.* **67** (2016) 1–34.

[24] R.H. Chisholm, T. Lorenzi and A. Lorz, Effects of an advection term in nonlocal lotka–volterra equations. *Commun. Math. Sci.* **14** (2016) 1181–1188.

[25] R.H. Chisholm, T. Lorenzi, A. Lorz, A.K. Larsen, L.N. De Almeida, A. Escargueil and J. Clairambault, Emergence of drug tolerance in cancer cell populations: an evolutionary outcome of selection, nongenetic instability and stress-induced adaptation. *Cancer Res.* **75** (2015) 930–939.

[26] H. Cho and D. Levy, Modeling the dynamics of heterogeneity of solid tumors in response to chemotherapy. *Bull. Math. Biol.* **79** (2017) 2986–3012.

[27] H. Cho and D. Levy, Modeling the chemotherapy-induced selection of drug-resistant traits during tumor growth. *J. Theor. Biol.* **436** (2018) 120–134.

[28] D.D. De Carvalho, S. Sharma, J.S. You, S.-F. Su, P.C. Taberlay, T.K. Kelly, X. Yang, G. Liang and P.A. Jones, DNA methylation screening identifies driver epigenetic events of cancer cell survival. *Cancer Cell* **21** (2012) 655–667.

[29] M. Delitala and T. Lorenzi, A mathematical model for the dynamics of cancer hepatocytes under therapeutic actions. *J. Theor. Biol.* **297** (2012) 88–102.

[30] M. Esteller, Epigenetics in cancer. *N. Engl. J. Med.* **358** (2008) 1148–1159.

[31] N. Eymard, V. Volpert, P. Kurbatova, V. Volpert, N. Bessonov, K. Ogungbenro, L. Aarons, P. Janiaud, P. Nony, A. Bajard, et al., Mathematical model of t-cell lymphoblastic lymphoma: disease, treatment, cure or relapse of a virtual cohort of patients. *Math. Med. Biol.* **35** (2016) 25–47.

[32] A.P. Feinberg, M.A. Koldobskiy and A. Göndör, Epigenetic modulators, modifiers and mediators in cancer aetiology and progression. *Nat. Rev. Genet.* **17** (2016) 284.

[33] A.P. Feinberg and B. Tycko, The history of cancer epigenetics. *Nat. Rev. Cancer* **4** (2004) 143.

[34] L.C. Franssen, T. Lorenzi, A.E. Burgess and M.A. Chaplain, A mathematical framework for modelling the metastatic spread of cancer. *Bull. Math. Biol.* (2018) 1–46.

[35] A. Ganesan, Epigenetic drug discovery: a success story for cofactor interference. *Philos. Trans. R. Soc. B: Biol. Sci.* **373** (2018) 20170069.

[36] R.A. Gatenby and P.K. Maini, Mathematical oncology: cancer summed up. *Nature* **421** (2003) 321.

[37] R.A. Gatenby, A.S. Silva, R.J. Gillies and B.R. Frieden, *Adaptive therapy. Cancer Res.* **69** (2009) 4894–4903.

[38] R. Glasspool, J.M. Teodoridis and R. Brown, Epigenetics as a mechanism driving polygenic clinical drug resistance. *Br. J. Cancer* **94** (2006) 1087–1092.

[39] M. Greaves and C.C. Maley, Clonal evolution in cancer. *Nature* **481** (2012) 306–313.

[40] S. Hamis, P. Nithiarasu and G.G. Powathil, What does not kill a tumour may make it stronger: in silico insights into chemotherapeutic drug resistance. *J. Theor. Biol.* **454** (2018) 253–267.

[41] S. Heerboth, K. Lapinska, N. Snyder, M. Leary, S. Rollinson and S. Sarkar, Use of epigenetic drugs in disease: an overview. *Genet. Epigenet.* **6** (2014) 9.

[42] G. Housman, S. Byler, S. Heerboth, K. Lapinska, M. Longacre, N. Snyder and S. Sarkar, Drug resistance in cancer: an overview. *Cancers* **6** (2014) 1769–1792.

[43] S. Huang, Genetic and non-genetic instability in tumor progression: link between the fitness landscape and the epigenetic landscape of cancer cells. *Cancer Metas. Rev.* **32** (2013) 423–448.

[44] P.A. Jones and P.W. Laird, Cancer-epigenetics comes of age. *Nat. Genet.* **21** (1999) 163.

[45] M.R. Junttila and F.J. de Sauvage, Influence of tumour micro-environment heterogeneity on therapeutic response. *Nature* **501** (2013) 346–354.

[46] K.S. Korolev, J.B. Xavier and J. Gore, Turning ecology and evolution against cancer. *Nat. Rev. Cancer* **14** (2014) 371.

[47] S. Kumar, R.K. Srivastav, D.W. Wilkes, T. Ross, S. Kim, J. Kowalski, S. Chatla, Q. Zhang, A. Nayak, M. Guha, *et al.*, Estrogen-dependent dll1-mediated notch signaling promotes luminal breast cancer. *Oncogene* (2018) 1.

[48] P. Kurbatova, S. Bernard, N. Bessonov, F. Crauste, I. Demin, C. Dumontet, S. Fischer and V. Volpert, Hybrid model of erythropoiesis and leukemia treatment with cytosine arabinoside. *SIAM J. Appl. Math.* **71** (2011) 2246–2268.

[49] A.A. Lane and B.A. Chabner, Histone deacetylase inhibitors in cancer therapy. *J. Clin. Oncol.* **27** (2009) 5459–5468.

[50] O. Lavi, J.M. Greene, D. Levy and M.M. Gottesman, The role of cell density and intratumoral heterogeneity in multidrug resistance. *Cancer Res.* **73** (2013) 7168–7175.

[51] O. Lavi, J.M. Greene, D. Levy and M.M. Gottesman, Simplifying the complexity of resistance heterogeneity in metastasis. *Trends Molec. Med.* **20** (2014) 129–136.

[52] T. Lorenzi, R.H. Chisholm and J. Clairambault, Tracking the evolution of cancer cell populations through the mathematical lens of phenotype-structured equations. *Biol. Direct* **11** (2016) 43.

[53] T. Lorenzi, R.H. Chisholm, L. Desvillettes and B.D. Hughes, Dissecting the dynamics of epigenetic changes in phenotype-structured populations exposed to fluctuating environments. *J. Theor. Biol.* **386** (2015) 166–176.

[54] T. Lorenzi, C. Venkataraman, A. Lorz and M.A. Chaplain, The role of spatial variations of abiotic factors in mediating intratumour phenotypic heterogeneity. *J. Theor. Biol.* **451** (2018) 101–110.

[55] A. Lorz, T. Lorenzi, J. Clairambault, A. Escargueil and B. Perthame, Modeling the effects of space structure and combination therapies on phenotypic heterogeneity and drug resistance in solid tumors. *Bull. Math. Biol.* **77** (2015) 1–22.

[56] A. Lorz, T. Lorenzi, M.E. Hochberg, J. Clairambault and B. Perthame, Populational adaptive evolution, chemotherapeutic resistance and multiple anti-cancer therapies. *ESAIM: M2AN* **47** (2013) 377–399.

[57] D.E. Matei and K.P. Nephew, Epigenetic therapies for chemoresensitization of epithelial ovarian cancer. *Gynecolog. Oncol.* **116** (2010) 195–201.

[58] L.M. Merlo, J.W. Pepper, B.J. Reid and C.C. Maley, Cancer as an evolutionary and ecological process. *Nat. Rev. Cancer* **6** (2006) 924–935.

[59] J. Miller, Parabolic cylinder functions, in Handbook of Mathematical Functions, U.S. Government Printing Office, Washington, DC (1964) 686–720.

[60] R.L. Momparler, Cancer epigenetics. *Oncogene* **22** (2003) 6479.

[61] P.C. Nowell, The clonal evolution of tumor cell populations. *Science* **194** (1976) 23–28.

[62] A. Olivier and C. Pouchol, Combination of direct methods and homotopy in numerical optimal control: application to the optimization of chemotherapy in cancer. *J. Optim. Theory Appl.* (2018).

[63] J. Otwinowski and J.B. Plotkin, Inferring fitness landscapes by regression produces biased estimates of epistasis. *Proc. Natl. Acad. Sci.* **111** (2014) E2301–E2309.

[64] P. Peltomäki, Mutations and epimutations in the origin of cancer. *Exp. Cell Res.* **318** (2012) 299–310.

[65] B. Perthame, Transport equations in biology, Birkhäuser, Basel, 2006.

[66] S.X. Pfister and A. Ashworth, Marked for death: targeting epigenetic changes in cancer. *Nat. Rev. Drug Disc.* **16** (2017) 241.

[67] G. Piazzi, L. Fini, M. Selgrad, M. Garcia, Y. Daoud, T. Wex, P. Malfertheiner, A. Gasbarrini, M. Romano, R.L. Meyer et al.. *Epigenetic regulation of delta-like controls notch activation in gastric cancer. Oncotarget* **2** (2011) 1291.
[68] A. Pisco and S. Huang, Non-genetic cancer cell plasticity and therapy-induced stemness in tumour relapse:'what does not kill me strengthens me'. *Br. J. Cancer* **112** (2015) 1725–1732.
[69] A.O. Pisco, A. Brock, J. Zhou, A. Moor, M. Mojtahedi, D. Jackson and S. Huang, Non-darwinian dynamics in therapy-induced cancer drug resistance. *Nat. Commun.* **4** (2013) 2467.
[70] F.J. Poelwijk, D.J. Kiviet, D.M. Weinreich and S.J. Tans, *Empirical fitness landscapes reveal accessible evolutionary paths. Nature* **445** (2007) 383.
[71] C. Pouchol, J. Clairambault, A. Lorz and E. Trélat, Asymptotic analysis and optimal control of an integro-differential system modelling healthy and cancer cells exposed to chemotherapy. *J. Math. Pures Appl.* **116** (2018) 268–308.
[72] Y. Pu, F. Zhao, H. Wang and S. Cai, Mir-34a-5p promotes multi-chemoresistance of osteosarcoma through down-regulation of the dll gene. *Sci. Reports* **7** (2017) 44218.
[73] D.F. Quail and J.A. Joyce, Microenvironmental regulation of tumor progression and metastasis. *Nat. Med.* **19** (2013) 1423–1437.
[74] S. Sarkar, G. Horn, K. Moulton, A. Oza, S. Byler, S. Kokolus and M. Longacre, Cancer development, progression and therapy: an epigenetic overview. *Int. J. Mol. Sci.* **14** (2013) 21087–21113.
[75] P. Schofield, M. Chaplain and S. Hubbard, Mathematical modelling of host–parasitoid systems: effects of chemically mediated parasitoid foraging strategies on within-and between-generation spatio-temporal dynamics. *J. Theor. Biol.* **214** (2002) 31–47.
[76] P.G. Schofield, M.A. Chaplain and S.F. Hubbard, Dynamic heterogeneous spatio-temporal pattern formation in host-parasitoid systems with synchronised generations. *J. Math. Biol.* **50** (2005) 559–583.
[77] A. Sharma, E.Y. Cao, V. Kumar, X. Zhang, H.S. Leong, A.M.L. Wong, N. Ramakrishnan, M. Hakimullah, H.M.V. Teo, F.T. Chong et al., Longitudinal single-cell RNA sequencing of patient-derived primary cells reveals drug-induced infidelity in stem cell hierarchy. *Nat. Commun.* **9** (2018) 4931.
[78] S. Sharma, T.K. Kelly and P.A. Jones, Epigenetics in cancer. *Carcinogenesis* **31** (2010) 27–36.
[79] S.V. Sharma, D.Y. Lee, B. Li, M.P. Quinlan, F. Takahashi, S. Maheswaran, U. McDermott, N. Azizian, L. Zou, M.A. Fischbach, et al., A chromatin-mediated reversible drug-tolerant state in cancer cell subpopulations. *Cell* **141** (2010) 69–80.
[80] A.S. Silva, Y. Kam, Z.P. Khin, S.E. Minton, R.J. Gillies and R.A. Gatenby, Evolutionary approaches to prolong progression-free survival in breast cancer. *Cancer Res.* **72** (2012) 6362–6370.
[81] V. Singh, P. Sharma and N. Capalash, DNA methyltransferase-1 inhibitors as epigenetic therapy for cancer. *Curr. Cancer Drug Targets* **13** (2013) 379–399.
[82] G. Steel and L. Lamerton, The growth rate of human tumours. *Br. J. Cancer* **20** (1966) 74.
[83] Y. Tamori and W.-M. Deng, Cell competition and its implications for development and cancer. *J. Genetics Genom.* **38** (2011) 483–495.
[84] N. Temme, Parabolic cylinder functions, NIST Handbook of Mathematical Functions (2010) 303–319.
[85] F. Thomas, D. Fisher, P. Fort, J.-P. Marie, S. Daoust, B. Roche, C. Grunau, C. Cosseau, G. Mitta, S. Baghdiguian, et al., Applying ecological and evolutionary theory to cancer: a long and winding road. *Evol. Appl.* **6** (2013) 1–10.
[86] O. Trédan, C.M. Galmarini, K. Patel and I.F. Tannock, Drug resistance and the solid tumor microenvironment. *J. Natl. Cancer Inst.* **99** (2007) 1441–1454.
[87] H.-C. Tsai and S.B. Baylin, Cancer epigenetics: linking basic biology to clinical medicine. *Cell Res.* **21** (2011) 502.
[88] L. Wagstaff, G. Kolahgar and E. Piddini, Competitive cell interactions in cancer: a cellular tug of war. *Trends Cell Biol.* **23** (2013) 160–167.
[89] C.B. Yoo and P.A. Jones, Epigenetic therapy of cancer: past, present and future. *Nat. Rev. Drug Discov.* **5** (2006) 37–50.
[90] H. Zhang, S. Pandey, M. Travers, H. Sun, G. Morton, J. Madzo, W. Chung, J. Khowsathit, O. Perez-Leal, C.A. Barrero, et al., Targeting cdk9 reactivates epigenetically silenced genes in cancer. *Cell* **175** (2018) 1244–1258.